EUROPEAN ORGANIZATION FOR NUCLEAR RESEARCH

CERN-PPE/92-102
01.06.1992

MUOPRODUCTION OF J/ψ AND THE GLUON DISTRIBUTION OF THE NUCLEON

The European Muon Collaboration

Aachen[1], *CERN*[2], *Freiburg*[3], *Max-Planck-Institut für Kernphysik Heidelberg*[4+], *Lancaster*[5], *LAPP (Annecy)*[6], *Liverpool*[7], *Marseille*[8], *Mons*[9], *Oxford*[10], *RAL (Chilton)*[11], *Sheffield*[12], *Torino*[13], *Uppsala*[14], *Institute for Nuclear Studies, Warsaw*[15++], *Warsaw*[16+++], *Wuppertal* [17], *Yale*[18]

J. Ashman[12], B. Badelek[16a)], G. Baum[18b)], J. Beaufays[2c)], C.P. Bee[7], C. Benchouk[8], I.G. Bird[5d)], S.C. Brown[7e)], M.C. Caputo[18f)], H.W.K. Cheung[10g)], J.S. Chima[11h)], J. Ciborowski[16a)], R. Clifft[11], G.Coignet[6], F. Combley[12], G. Court[7], G. d'Agostini[8], J. Drees[17], M. Düren[1], N. Dyce[5], A.W. Edwards[17i)], M. Edwards[11], T. Ernst[3], M.I. Ferrero[13], D. Francis[7], E. Gabathuler[7], J. Gajewski[16], R. Gamet[7], V. Gibson[10j)], J. Gillies[10k)], P. Grafström[14l)], K. Hamacher[17], D.von Harrach[4m)], P. Hayman[7], J.R. Holt[7], V.W. Hughes[18], A. Jacholkowska[2n)], T. Jones[7], E.M. Kabuss[4m)], B. Korzen[17], U. Krüner[17], S. Kullander[14], U. Landgraf[3], D. Lanske[1], F. Lettenström[14o)], T. Lindqvist[14], M. Matthews[7], Y. Mizuno[4p)], K. Mönig[17], F. Montanet[8], J. Nassalski[15q)], T. Niinikoski[2], P.R. Norton[11], F.G. Oakham[11r)], R.F. Oppenheim[18s)], A.M. Osborne[2], V. Papavassiliou[18], N. Pavel[17t)], C. Peroni[13], H. Peschel[17u)], R. Piegaia[18f)], B. Pietrzyk[8], B. Povh[4], P. Renton[10], J.M. Rieubland[2], K. Rith[4], E. Rondio[16a)], L. Ropelewski[16a)], D. Salmon[12k)], A. Sandacz[15q)], T. Schröder[3], K.P. Schüler[18], K. Schultze[1], T.- A. Shibata[4], T. Sloan[5], A. Staiano[13], H.E. Stier[3], J. Stock[3], G.N. Taylor[10v)], J.C. Thompson[11], T. Walcher[4m)], J.Toth[6w)], L. Urban[1], L. Urban[6w)], W. Wallucks[3], S. Wheeler[12l)], W.S.C. Williams[10], S.J. Wimpenny[7x)], R. Windmolders[9], J. Womersley[10y)], K. Ziemons[1]

(Submitted to Z. Phys. C)

Abstract

Measurements are presented of the inclusive distributions of the J/ψ meson produced by muons of energy 200 GeV from an ammonia target. The gluon distribution of the nucleon has been derived from the data in the range $0.04 < x < 0.36$ using a technique based on the colour singlet model. An arbitrary normalisation factor is required to obtain a reasonable integral of the gluon distribution. Some comments are made on the use of J/ψ production by virtual photons to extract the gluon distribution at HERA.

For footnotes see next page

+ Supported by Bundesministerium für Forschung und Technologie.
++ Supported by CPBP.01.06
+++Supported by CPBP.01.09
a) University of Warsaw, Poland, partly supported by CPBP-01.06.
b) Permanent address, University of Bielefeld, FRG.
c) Now at TRASYS, Brussels, Belgium.
d) Now at NIKHEF-K, AJ Amsterdam, The Netherlands.
e) Now at TESA, S.A., Renens, Switzerland.
f) Now at City University, Buenos Aires, Argentina.
g) Now at University of Colarado, Boulder, Colarado, USA.
h) Now at British Telecom, London, UK.
i) Now at Jet, Joint Undertaking, Abingdon, UK.
j) Now at University of Cambridge, Cambridge, UK.
k) Now at R.A.L., Chilton, Didcot, U.K.
l) Now at CERN, Geneva, Switzerland.
m) Now at University of Mainz, Mainz, FRG.
n) Now at L.A.L., Orsay, France.
o) Now at University of California, Santa Cruz, USA.
p) Now at Osaka University, Osaka, Japan.
q) Permanent address, Institute for Nuclear Studies, Warsaw, Poland.
r) Now at NRC, Ottawa, Canada.
s) Now at AT&T, Bell Laboratories, Naperville, Illinois, U.S.A.
t) Now at University of Hamburg, Hamburg, FRG
u) Now at Gruner and Jahr AG, Itzehoe, FRG.
v) Now at University of Melbourne, Parkville, Victoria, Australia.
w) Permanent address: Central Research Institute for Physics, Budapest, Hungary.
x) Now at University of California, Riverside, U.S.A.
y) Now at University of Florida, Gainesville, U.S.A.

Addresses
1) III Physikalisches Institut A, Physikzentrum, RWTH, D-5100 Aachen, FRG.
2) CERN, CH-1211 Geneva 23, Switzerland.
3) Fakult
4) Max-Planck Institut für Kernphysik, 6900 Heidelberg, FRG.
5) Department of Physics, University of Lancaster, Lancaster LA1 4YB, UK.
6) Laboratoire d'Annecy-le-Vieux de Physique des Particules, BP110, F-74019 Annecy-le-Vieux, Cedex, France.
7) Department of Physics, University of Liverpool, Liverpool L69 3BX, UK.
8) Centre de Physique des Particules, Faculté des Sciences de Luminy, F-13288 Marseille, France.
9) Faculté des Sciences, Université de Mons, B-7000 Mons, Belgium.
10) Nuclear Physics Laboratory, University of Oxford, Oxford OX1 3RH, UK.
11) Rutherford and Appleton Laboratory, Chilton, Didcot OX1 0QX, UK. 12) Department of Physics, University of Sheffield, Sheffield S3 7RH, UK.
13) Istituto di Fisica, Universitá di Torino, I-10125, Italy.
14) Department of Radiation Science, University of Uppsala, S- 75121 Uppsala, Sweden.
15) Institute for Nuclear Studies, 00681JWarsaw, Poland.
16. Physics Institute, University of Warsaw.
17) Fachbereich Physik, Universität Wuppertal, D-5600 Wuppertal, FRG.
18) Physics Department, Yale University, New Haven, Connecticut, USA.

1. Introduction

The production cross section for J/ψ mesons by virtual photons has long been thought to be related to the gluon distribution of the nucleon since the process is believed to proceed through the fusion of a photon and a gluon via an intermediate charm-anticharm quark pair[1,2,3]. A method has been proposed [4] to extract this gluon distribution using the colour singlet model for J/ψ photoproduction [5]. This method was suggested explicitly for the kinematic region of future experiments at HERA [6]. In this paper measurements of J/ψ production by 200 GeV positive muons from an ammonia target are described. The measured inclusive J/ψ distributions are presented and used to define the kinematic region of validity for the method of [4], which is based on perturbative QCD. The method is then used to attempt to extract the gluon distribution of the nucleon. Some observations which are relevant to the determination of this at HERA will be made. Further details of the analysis are described in [7]. A similar analysis of the NMC J/ψ data from hydrogen and deuterium targets has already been described [8,9].

2. Experimental Method

The experiment was performed in the M2 muon beam line at the CERN SPS using the EMC forward spectrometer[10] to detect the scattered muon, the fast forward hadrons and decay muons produced in deep inelastic scattering. The spectrometer and the analysis procedures for this phase of the experiment have already been described [11,12]. The small multiwire proportional chambers (labelled P0A,P0B,P0C,P0D and P0E in fig 1 of [12]) were installed in the beam region to cover the deadened areas of the other wire chambers. These were essential for the analysis presented here since the apparatus was triggered predominantly by the decay muons from the J/ψ, the scattered muon being detected mainly in the P0 chamber system.

The target was the 80 cm long polarised target used to study the spin dependence of the proton structure function [11,12], summing the J/ψ data over the opposite spin alignments. It consisted mainly of ammonia with a small admixture of helium (10% by weight) having a

mean atomic weight of 10.8. Other thinner targets, located about 1m downstream [13], were not used in this analysis. The data were taken in five separate running periods at the SPS with positive incident muons of energy 200 GeV. The J/ψ yields per period were consistent within the statistical errors and the data were averaged over all the experimental runs.

3. Data Reduction

The data were passed through a chain of analysis programmes in which pattern recognition, track and vertex reconstruction were carried out[12]. Events initially reconstructed with a $\mu^+\mu^-$ pair (90% of the sample) or $\mu^+\mu^+\mu^-$ (10% of the sample), which were consistent with having satisfied the trigger requirements, were selected for further analysis. Cuts were applied to the longitudinal vertex position to ensure that the candidate events originated in the polarised target cells and small corrections (5%) were applied for events smeared by resolution outside these cuts. Fig. 1 (dashed histogram) shows the invariant mass distribution of all resulting $\mu^+\mu^-$ pairs in which the muon momenta are greater than 10 GeV. A clear peak at the J/ψ mass can be seen on a background mainly from deep inelastic scattering events in which the μ^+ is the scattered muon and the μ^- originates from the decay of a π^- or K^-.

For the sample of $\mu^+\mu^-$ pairs (90% of the total) the third muon in the event was searched for in the P0 chamber system from the reconstructed vertex position and the observed hits in the P0 chambers. The method of principal components was employed using the CERN programmme LINTRA[14] followed by momentum fitting with the programme MUDIFI[15]. The muon found by this procedure was assumed to be the scattered muon in the event i.e. the originator of the virtual photon. In the sample of $\mu^+\mu^+\mu^-$ events (10% of the total) found by the initial analysis chain the scattered muon was assumed to be the faster positive muon unless it could be combined with the μ^- to produce an event in the J/ψ mass peak.

The solid histogram in fig. 1 shows the $\mu^+\mu^-$ mass spectrum for all events in which the third muon was successfully found. The background under the J/ψ peak is reduced considerably compared to that observed when the third muon is not found with only a small reduction in the J/ψ mass peak. Fits of a Gaussian peak plus a smooth background function

were performed to the data in fig. 1 in the range $2.0 < M_{\mu\mu} < 4.5$ GeV. The mass of the J/ψ was found to be 3096.9 $\pm$ 2.5 MeV, in good agreement with the Particle Data Table [16]. The ratio of the number of J/ψ events in the solid histogram (from the area of the gaussian peak) to that in the dashed histogram was (70.3 $\pm$ 4.2)%. This was taken to be the efficiency of the P0 track finding procedure and all cross sections are corrected for this inefficiency. The continuum in the mass spectrum below the J/ψ mass in the solid histogram (fig. 1) is thought to originate mainly from QED processes such as trident production.

For this analysis, the standard variables of deep inelastic scattering are defined in table I. To compute the apparatus acceptance a Monte Carlo simulation was used. This requires an input generator for J/ψ mesons which was deduced from the data as follows. The measured event distributions in Q^2, ν, Z and P_t^2 were used to generate an initial sample of Monte Carlo events, from which the acceptance corrections for the data were derived. The corrected data distributions were then used to generate the next sample of Monte Carlo events, from which the acceptance corrections were re-evaluated. The process was iterated until the changes in the corrected distributions were small and the ratios of the data to the Monte Carlo distributions were flat. Four such iterations were needed. The distributions of the decay angles of the J/ψ, were assumed to be uniform throughout. The earlier EMC [3] and the NMC [9] measurements show that this is approximately true at low Z and high P_t as expected theoretically[17]. This may not be the case in the diffractive region. The acceptance changed by 16% if a $1 + \cos^2\theta$ decay angular distribution is used rather than a flat distribution and this is taken to be a contribution to the normalisation systematic error. Here θ is the polar angle of the decay muon from the J/ψ relative to the line of flight of the J/ψ in its rest frame.

An additional kinematic cut, demanding $50 < \nu < 180$ GeV, was applied to the data to reject regions of small or rapidly varying acceptance. The number of J/ψ events satisfying all cuts was 274. Fig. 2 shows the acceptance as a function of the kinematic variables for the final sample. The spike in the acceptance in Z can be understood in terms of resolution smearing. Events with $Z > 1.1$ are rejected and the remaining events with $Z > 1.0$ are folded over into the upper Z bins. Events in the bin $0.95 \leq z < 1.0$ are smeared down into

the bin $0.9 < z < 0.95$ with comparatively few smeared in the opposite direction because of better measurement resolution at lower Z and smaller cross sections. Hence the acceptance correction is rather different for the bin $0.9 < Z < 0.95$ than it is for $0.95 < Z < 1.0$.

The number of J/ψ events in each kinematic bin was obtained from the range 2.975 $< M_{\mu\mu} <$ 3.2 GeV. The backgrounds under the peak in each bin ($< 7\%$) were estimated from the numbers of events in control regions on each side of the peak ($2.0 < M_{\mu\mu} < 2.875$ GeV and $3.3 < M_{\mu\mu} < 4.5$ GeV) normalised to the J/ψ mass range. The cross sections in each bin were deduced from the event yields, the target thickness (39.4 gms/cm^2), the number of incident muons within the beam phase space [18] ($30.9 \pm 0.8 \times 10^{11}$) and the branching ratio of J/$\psi \rightarrow \mu^+\mu^-$ (0.069 [16]). Radiative corrections were applied using the procedure of Mo and Tsai [19] with a parameterisation of the cross sections for J/ψ production measured in [3]. These corrections were always less than 10%. The reconstruction efficiency for each decay muon was estimated to be $88 \pm 6\%$ [20] where the uncertainty is derived from the variation amongst different methods used to estimate it. Combining this error with the uncertainty in the P0 track reconstruction software (6.0%), the uncertainty in the number of incident muons (2.6%) and that due to lack of knowledge of the precise decay angular distribution of the J/ψ (16%), gives together with the error in the J/$\psi \rightarrow \mu^+\mu^-$ branching ratio [16] (13%) an overall normalisation systematic error of 23%.

4. Results

4.1 The Measured Cross Section

Following the procedure in [3] the cross sections were measured as a function of Q^2 and fits were made of a propagator form $\sigma(Q^2 = 0)/\left(1 + \frac{Q^2}{M^2}\right)^2$. The value of the J/$\psi$ photoproduction cross section, $\sigma\ (Q^2 = 0)$, was found to be 36 $\pm$3(stat) $\pm$7 (syst) nb. Table II gives the measured cross sections as a function of Z and P_t^2, and these are shown in fig. 3 and compared to the data of [3]. There is reasonable agreement over most of the kinematic range. However, at low P_t^2 and high Z the data from [3] tend to lie above those presented here. In the highest Z and lowest P_t^2 bin this arises from the stronger coherent production

from the larger target iron nucleus of [3] than for the nuclei of ammonia (NH_3) used in this experiment. The excess signal in [3] at low P_t^2 for $0.95 > Z > 0.8$ arises from the smearing of the coherently produced events due to the rather poor resolution in that experiment [3] which had a thick calorimeter target. Thus at least part of the excess signal in the production of J/ψ from iron compared to deuterium reported in [21] is probably due to such smearing of the coherent signal. Recently NMC[22] have reported a slight excess signal in J/ψ production from tin with respect to carbon which may arise from excess gluons in the heavier nucleus.

The data in fig. 3 were integrated over P_t^2 to obtain the photoproduction ($Q^2 = 0$) cross section, $\frac{d\sigma}{dZ}$, shown in fig. 4. Comparison is made with other measurements. There are some differences between the measurements due, in part, to the different selection procedures and coherent contributions in each experiment. However, the trend of the data is clear. The dashed curve shows the prediction of a higher order photon gluon fusion calculation by Duke and Owens [23] and the dash-dotted curve shows the predictions of the colour singlet model of Berger and Jones [5]. The normalisation of these curves is arbitrary. For $Z < 0.9$ the data favour the shallower Z variation preferred by the colour singlet model to the much steeper dependence predicted by the Duke and Owens model. The latter model has many graphs involving gluon bremsstrahlung and the steep Z variation predicted seems to be favoured for $Z > 0.9$ in the approach to the diffractive region.

A potentially large source of background in J/ψ production in the inelastic region could come from elastic and inelastic ψ' production with decay to J/ψ $\pi\pi$ (branching ratio 55% [16]). The total cross section for ψ' production has been measured to be 20% of that for J/ψ [3,9,24]. This background is difficult to assess since the ψ' distributions have never been measured. A Monte Carlo simulation of ψ' production was made, assuming that the ψ' distributions are identical to those of the J/ψ and normalising the total cross section to the measured value. The background from ψ' production, using this simulation, was found to vary between 0-40% over the $Z - P_t^2$ region of this experiment (fig. 3). The data in figs. 3 and 4 are not corrected for this background.

4.2 The Gluon Distribution of the Nucleon

The method used to obtain the gluon distribution of the target nucleon, $G(x,\hat{Q}^2)$, is to divide the measured J/ψ production cross section by the cross section for the production of the J/ψ from photon-gluon scattering, calculated by perturbative QCD from the colour singlet model [5]. In this model (with $\hbar = c = 1$) the cross section for J/ψ production by real photons ($Q^2 = 0$) from a nucleon is given by

$$\frac{d^2\sigma}{dZdP_t^2} = \frac{128\pi^2 G(x,\hat{Q}^2) m_\psi \alpha_s^2 \alpha e_q^2 |R_s(0)|^2}{3s[m_\psi^2(1-Z)+P_t^2]} \left[\frac{1}{M_T^4} + \frac{(1-Z)^4}{K_T^4} + \frac{Z^4 P_t^4}{M_T^4 K_T^4}\right] \tag{1}$$

with

$$M_T^2 = m_\psi^2 + P_t^2 \text{ and } K_T^2 = m_\psi^2(1-Z)^2 + P_t^2 \tag{2}$$

Here m_ψ is the mass of the J/ψ, α and α_s the QED and QCD coupling constants, respectively and e_q is the electric charge of the charmed quark. The J/ψ radial wave function at the origin, $R_s(0)$, is determined from the observed leptonic width using

$$\Gamma(J/\psi \rightarrow ee) = 16\pi\alpha^2 e_q^2 |R_s(0)|^2/m_\psi^2 = 4.7KeV. \tag{3}$$

$\hat{Q}^2$, the energy scale probed is taken to be m_ψ^2 and x, the fraction of the momentum of the target nucleon carried by the initial state gluon is given by

$$x = \frac{\hat{s}}{s} = \frac{1}{s}\left[\frac{m_\psi^2}{Z} + \frac{P_t^2}{(1-Z)Z}\right] \tag{4}$$

where $\sqrt{s}$ is the photon-nucleon and $\sqrt{\hat{s}}$ the photon-gluon centre of mass energy, respectively.

Following the suggestion of Martin, Ng and Stirling [4] we compute the muon-gluon cross section for $\mu g \rightarrow$J/ψ g using equation (1) setting the gluon density term $G(x,\hat{Q}^2)$ to unity. Since we are computing a muoproduction cross section, equation (1) is multiplied by the virtual flux factor [33] and a propagator term $\frac{1}{\left(1+\frac{Q^2}{M^2}\right)^2}$. The accuracy of such a formalism has been demonstrated [8,27]. The calculated cross sections are then integrated over the measured variables Q^2, ν, Z, P_t^2 in a fixed interval of x by Monte Carlo. The integrals are evaluated over the kinematic range covered by the data ($50 < \nu < 180$ GeV, $0.4 < Z < 0.95$,

$P_t^2 > 0.1$ GeV^2 and $Q^2_{min} < Q^2 < Q^2_{max}$ where Q^2_{min} and Q^2_{max} represent the kinematic limits).

The ranges in Z and P_t^2 were chosen to define an inelastic region in which the colour singlet model describes the data. Such a region must be free from diffractive and other non perturbative effects expected to occur at high Z and low P_t^2. This region was chosen by evaluating $xG(x,\hat{Q}^2)$ averaged over the whole x range, using various low P_t^2 and high Z cuts, and selecting the range in which $xG(x,\hat{Q}^2)$ is constant. Figure 5 shows the values of $xG(x,\hat{Q}^2)$ obtained. It can be seen that $xG(x,\hat{Q}^2)$ rises, if the inelastic region is extended too high in Z or too low in P_t^2, due to the onset of such non perturbative effects. The region of constant $xG(x,\hat{Q}^2)$ chosen was $Z < 0.95$ and $P_t^2 > 0.1$ GeV^2. After selecting this region 130 events remained. The measured Q^2 dependence of the cross section in this region has been fitted to the propagator form giving a propagator mass $M = 2.75 \pm 0.54$ GeV/c^2 which was used in the calculation of the integrals described above.

The data were then divided into four intervals of x and the cross sections and integrals were derived (see Table III). The integrals in Table III were calculated with $\alpha_s = 1.0$ rather than the accepted value $\alpha_s(m_\psi^2) = 0.3$ [16] since it was found to be necessary to apply an arbitrary normalisation factor, K^2. This can be seen from fig. 5 where the mean value of $xG(x,\hat{Q}^2)$ of 4.7 ± 0.5 computed with the standard value of α_s is larger than that expected from parameterisations of deep inelastic structure function measurements [28,29,30,31]. At the mean x of the data ($< x >= 0.13$) this is expected to be close to unity. Previous measurements [3,9] have also shown that the colour singlet model predicts cross sections lower than the data.

The arbitrary normalisation factor K^2 was determined from a fit of the form

$$xG(x,\hat{Q}^2) = (K\alpha_s)^2 \frac{n+1}{2}(1-x)^n$$

to the values of $xG(x,\hat{Q}^2)$. The value of $K\alpha_s$ was chosen so that $\int xG(x,\hat{Q}^2)dx = 0.5$, the known fraction of the nucleon's momentum carried by gluons [32]. The data in table III cover $\sim$ 70% of this integral. The fit gave $K\alpha_s = 0.71 \pm 0.04$(stat) ± 0.08(syst) and

$n = 5.7 \pm 1.5(\text{stat}) \pm 1.0(\text{ syst})$. The systematic errors were derived from a study [7] of the sensitivity of the fit to the cuts applied and to the assumed propagator mass. M. Taking $\alpha_s = 0.3$. the arbitrary normalisation factor is $K^2 = 5.6 \pm 0.6$ (stat) $\pm$ 1.3 (syst). The final column of table III gives the values of $xG(x, \hat{Q}^2)$ which include this arbitrary normalisation. Fig. 6 shows these values as a function of x together with the fit and the results from the NMC [9]. There is good agreement between the two sets of measurements. The data in fig. 6 are not corrected for the background from ψ' decays which, using the simulation of ψ' production described above, was estimated to be 20% of the measured cross section in the smallest x bin for this experiment, falling to 13% in the highest x bin.

The arbitrary normalisation factor reported in the NMC analysis [9] was 2.4 $\pm$ 0.4. However, they include in equation (1) the leading order QCD radiative correction factor to the leptonic width Γ_{ee} of $(1 - 16\alpha_s(M_\psi^2)/3\pi)$, suggested by Barbieri et al [34]. Applying such a correction, the arbitrary normalisation factor for the data reported here would be 2.7 $\pm$ 0.7, in good agreement with the NMC value.

Such large values of the normalisation factor cast some doubt on the validity of the procedure described to obtain the gluon distribution of the nucleon from the J/ψ photoproduction cross sections. Unless we know the reason for such a factor, the spectre of an x dependent effect which would bias the distribution obtained, hangs over the measurement. One is rather encouraged that the leading order QCD radiative correction[34] to the leptonic width of the J/ψ already explains half the discrepancy in normalisation between the colour singlet model and the data. This may mean that higher order corrections to the leptonic J/ψ width and to the colour singlet model could be important. The possibility of an x dependent effect would be eliminated if the residual normalisation factor could be explained by such higher order corrections, so removing any doubts. Such higher order effects have not yet been derived. Nevertheless, the gluon distributions obtained seem sensible. This is illustrated in fig. 7 where the data from fig. 6 are compared with recent parameterisations of the gluon structure function[28-31,35]. There is good agreement with all of the parameterisations of [28-30] which were made directly from deep inelastic scattering data. There is also reasonable

although somewhat poorer agreement with the dynamically generated parton distributions [31.36] (fig. 7d). This indicates that, despite the problems alluded to above, the J/ψ data give a reasonable estimate of the shape of the gluon structure function of the nucleon.

Conclusions

The Z and P_t^2 distributions in J/ψ muoproduction have been presented and used to derive the gluon distribution of the nucleon by the procedure suggested by Martin et al for higher energy data at HERA. The shape of the gluon distribution obtained shows reasonable agreement with those obtained from parameterisations of deep inelastic scattering data. This indicates that the procedure could be reliable. However, an arbitrary normalisation factor is required to obtain a reasonable value of the integral of the gluon distribution. A significant part of this normalisation factor can be explained by the leading order QCD radiative correction to the leptonic J/ψ width. However, before the procedure can be said to be a precision method of measuring the gluon distribution of the nucleon at HERA it should be ascertained whether or not the residual arbitrary normalisation factor is due to higher order QCD corrections in order to eliminate the possibility of an x dependent bias in the normalisation. In addition, measurements of the cross sections for ψ' production are needed to deduce the background in direct J/ψ production.

We thank M de Jong and C Mariotti for helpful comments.

Table I

Kinematic Variables

$k = (E, \mathbf{k})$	Incident muon 4-vector
$k' = (E', \mathbf{k}')$	Scattered muon 4-vector
$Q^2 = -q^2 = (k - k')^2$	Four momentum squared transferred to the virtual photon
$\nu = E - E'$	Energy transferred to the virtual photon
$Z = E_{J/\psi}/\nu$	Fraction of the energy of the virtual photon taken away by the J/ψ
P_t	Transverse momentum of the J/ψ relative to the virtual photon

Table II

The J/ψ differential virtual photoproduction cross sections ($Q^2 = 0$) $d^2\sigma/dZdP_t^2$ nb(GeV/c^2)$^{-2}$, normalised to a total cross section of 36 nb, (not corrected for coherence).

	P_t^2 (GeV/c^2)^2						
Z	0 -0.18	0.18 -0.32	0.32 -0.56	0.56 -1.0	1.0 -1.8	1.8 -3.2	3.2 -5.6
0.4-0.6	19.0 ± 9.8	11.9 ± 9.9	6.0 ± 4.4	4.7 ± 3.2	3.7 ± 2.0	1.5 ± 1.2	
0.6-0.7	21.2 ± 13.0	5.3 ± 5.5	13.7 ± 10.2	17.2 ± 7.3	7.2 ± 3.9	5.0 ± 2.9	
0.7-0.8	58.8 ± 21.0	17.7 ± 13.7	19.6 ± 12.2	9.9 ± 5.4	9.0 ± 4.4	7.5 ± 3.1	2.5 ± 2.4
0.8-0.9	24.2 ± 13.3	22.2 ± 13.5	15.7 ± 9.9	16.9 ± 8.1	8.8 ± 4.0	3.8 ± 1.9	0.6 ± 0.6
0.9-0.95	192.8 ± 45.8	70.3 ± 30.2	24.1 ± 12.6	23.2 ± 9.0	9.9 ± 4.8	6.4 ± 2.6	2.4 ± 3.4
0.95-1.0	1091.3 ± 149.2	231.9 ± 73.1	143.1 ± 42.2	160.2 ± 34.9	29.0 ± 10.6	6.5 ± 4.0	2.9 ± 2.3

Table III

The gluon densities

x range	$< x >$	$\frac{d\sigma}{dx}$ nb (data)	Integrals (computed from colour singlet model)	$xG(x)$ (normalised so that integral is 0.5)
0.044-0.0743	0.060	0.87±0.21	0.766	2.25±0.54
0.0743-0.125	0.098	1.21±0.17	1.196	1.99±0.29
0.125-0.210	0.162	0.47±0.09	0.871	1.09±0.22
0.210-0.359	0.259	0.085±0.023	0.257	0.67±0.19

References

1. T. Weiler, Phys. Rev. Lett. **44** (1980) 304.
   V. Barger, W.Y. Keung and R.J.N. Phillips, Phys. Lett. **91B** (1980) 253.
2. R. Baier and R. Rückl, Nucl. Phys. **B218** (1983) 289.
3. EMC; J.J. Aubert et al, Nucl. Phys. **B213** (1983) 1.
4. A.D. Martin, C.K. Ng and W.J. Stirling, Phys. Lett. **191B** (1987) 200.
5. E.L. Berger and D. Jones, Phys. Rev. **D23** (1981) 1521.
6. S.M. Tkaczyk, W.J. Stirling and D.H. Saxon, RAL-88-041.
   H. Jung, G.A. Schuler and J. Terron DESY preprint 92-028 (1992).
7. N. Dyce, PhD Thesis, University of Lancaster, (1988), RAL-T-073.
8. M. de Jong, PhD Thesis, Free University of Amsterdam (1991).
9. NMC, D. Allasia et al, Phys. Lett. **B258** (1991) 493.
10. EMC, O.C. Allkofer et al, Nucl. Inst. and Methods **179** (1981) 445.
11. EMC, J. Ashman et al, Phys. Lett. **206** (1988) 364.

12. EMC, J. Ashman et al, Nucl. Phys. **B328** (1989) 1.

13. EMC, J. Ashman et al, Phys. Lett. **202** (1988) 603.

14. R. Brun, M. Hansroul and J. Kubler, CERN DD/EE/79-5 (1980).

15. R. Brun, M. Hansroul and H. Wind, CERN DD/EE/80-1 (1981).

16. Particle Data Group, Review of Particle Properties, Phys. Lett. **239** (1990).

17. J.G. Körner, J. Cleymans, M. Kuroda and G.J. Gounaris, Nucl. Phys. **B204** (1982) 6.

18. R. Mount, Nucl. Inst. and Methods **187** (1981) 401.

19. L. Mo and Y.S. Tsai, Rev. Mod. Phys. **41** (1965) 205 and Y.S. Tsai SLAC-PUB-848 (1971).

20. H.W.K. Cheung, PhD Thesis, University of Oxford (1989), RAL-T-055.

21. EMC, J.J. Aubert et al, Phys. Lett. **152B** (1985) 433.

22. NMC, P. Amaudruz et al, Nucl. Phys. **B371** (1992) 553.

23. D.W. Duke and J.F. Owens, Phys. Lett. **96B** (1980) 184.

24. NA14, R. Barate et al, Z. Phys. C - Particles and Fields **C33** (1987) 505.

25. BFP, T.W. Markiewicz, PhD Thesis, Lawrence Berkeley Lab (1982) and M. Strovink, Proc. of 1981 International Symposium on Leptons and Photon Interactions, Bonn.

26. FTPS, B.H. Denby et al, Phys. Rev. Lett. **52** (1984) 795.

27. K.J. Abraham, Phys. Lett. B240 (1990) 224.

28. J. Kwiecinski, A.D. Martin, R.G. Roberts and W.J. Stirling, Phys. Rev. **D42** (1990) 3645 and P. Harriman, A.D. Martin, R.G. Roberts and W.J. Stirling, Phys. Rev. **D42** (1990) 798.

29. J. Morfin and W.K. Tung, Z. Phys. C - Particles and Fields **C52** (1992) 13.

30. M. Diemoz, F. Ferroni, E. Longo and G. Martinelli, Z. Phys. C - Particles and Fields **C39** (1988) 21.

31. M. Gluck, E. Reya and A. Vogt, Z. Phys. C - Particles and Fields **C53** (1992) 127.

32. T. Sloan, G. Smadja and R. Voss, Phys. Reports **162** (1988) 45.

33. L. Hand, Phys. Rev. **129** (1963) 1834. The transverse photon flux only is calculated since the longitudinal cross section is predicted to be small (T. Weiler, Phys. Rev. Lett. **44** (1980) 304).

34. R. Barbieri, R. Gatto and E. Remiddi, Phys. Lett. **106B** (1981) 497.

35. V. Barone, M. Genovese, N.N. Nikolaev, E. Predazzi and B.G. Zakharov, Preprint DFTT 8/92 (1992).

36. C. Mariotti, PhD Thesis, University of Torino (1992).

Figure Captions

Figure 1: The $\mu^+\mu^-$ invariant mass plot: dashed histogram. all $\mu^+\mu^-$ pairs; solid histogram, $\mu^+\mu^-$ pairs with the scattered muon found.

Figure 2: J/ψ Acceptance in the generated variables after kinematic cuts.

Figure 3: The photoproduction ($Q^2 = 0$) cross sections $d^2\sigma/dZdP_t^2$ from this experiment (open points) and the NA2 iron data[3] (solid points).

Figure 4: $d\sigma/dZ$ world data. The dash-dotted curve is the prediction of the colour singlet model [5], the dashed curve is $d^2\sigma/dZdP_t^2$ for $P_t^2 = 1$ GeV^2 predicted by [23]. Both curves are arbitrarily normalised. The data are from NA14[24], BFP[25], FTPS[26] EMC[3], and NMC[36]. The FTPS and NA14 data are inelastic only as demanded by the presence of other particle tracks in addition to the J/ψ .

Figure 5: $xG(x, \hat{Q}^2)$ averaged over all x as a function of the allowed maximum Z for different minimum P_t^2. It should be noted that the error bars are absolutely correlated since the data with lower maximum Z in each plot is a subsample of those with higher maximum Z.

Figure 6 The normalised gluon distribution, $xG(x, \hat{Q}^2)$ (table III) together with the NMC J/ψ data [9]. The curve is a fitted parameterisation of the data in table III .

Figure 7: The gluon distribution from the J/ψ data compared with parameterisations of the gluon structure function; a) DFLM[30], b) Morfin-Tung[29], (set 6 and set 3, the best and worst fits; c) HMRS and KMRS[28], (HMRSE and KMRSB-, the best and worst fits); d) GRV[31] and BGNPZ[35].

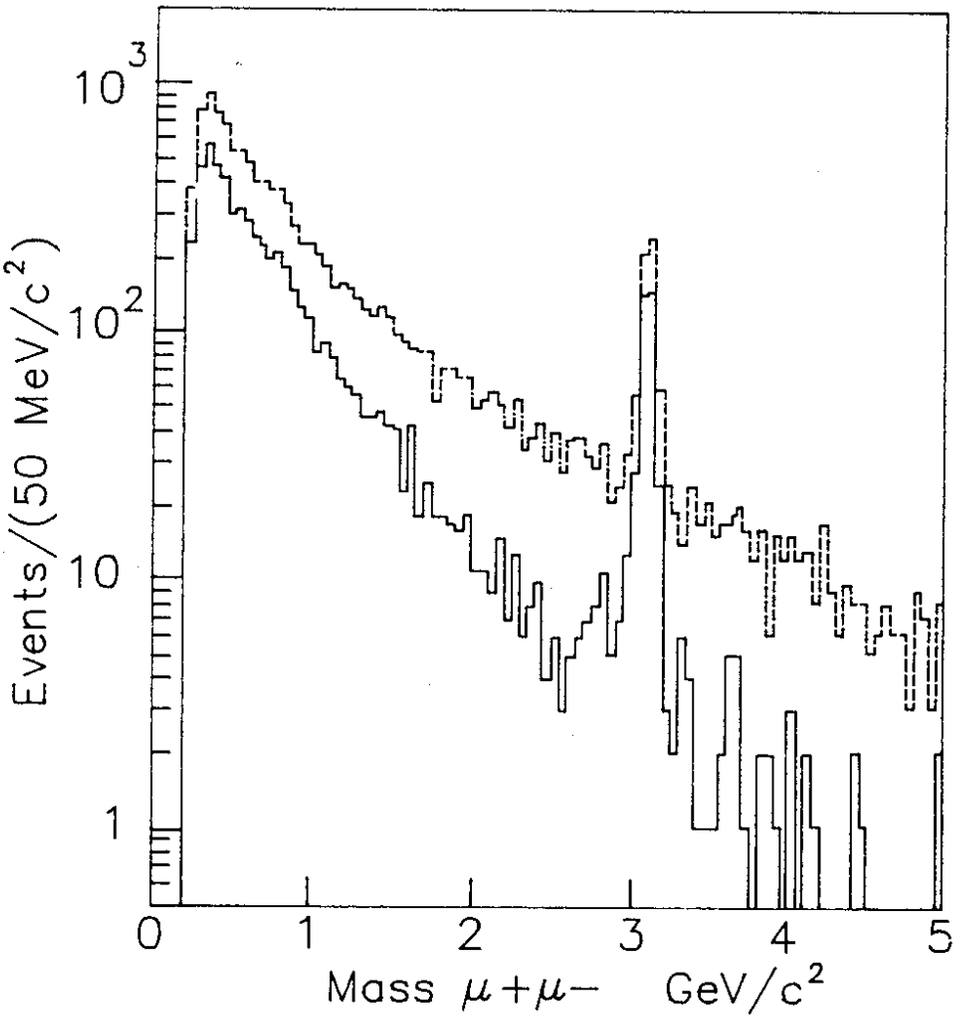

Fig. 1

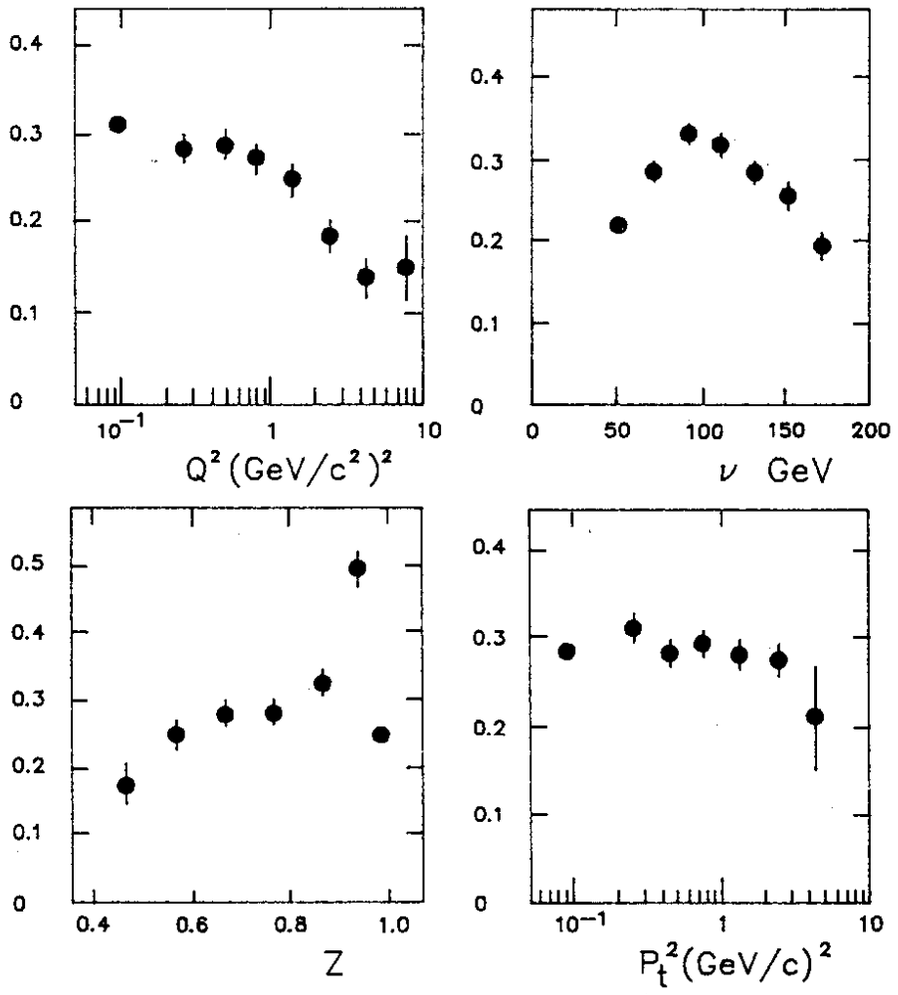
0.4
0.3
0.2
0.1
0
10^{-1}
1
10
$Q^2\,(GeV/c^2)^2$
0.4
0.3
0.2
0.1
0
0
50
100
150
200
ν GeV
0.5
0.4
0.3
0.2
0.1
0
0.4
0.6
0.8
1.0
Z
0.4
0.3
0.2
0.1
0
10^{-1}
1
10
$P_t^2\,(GeV/c)^2$

Fig.2

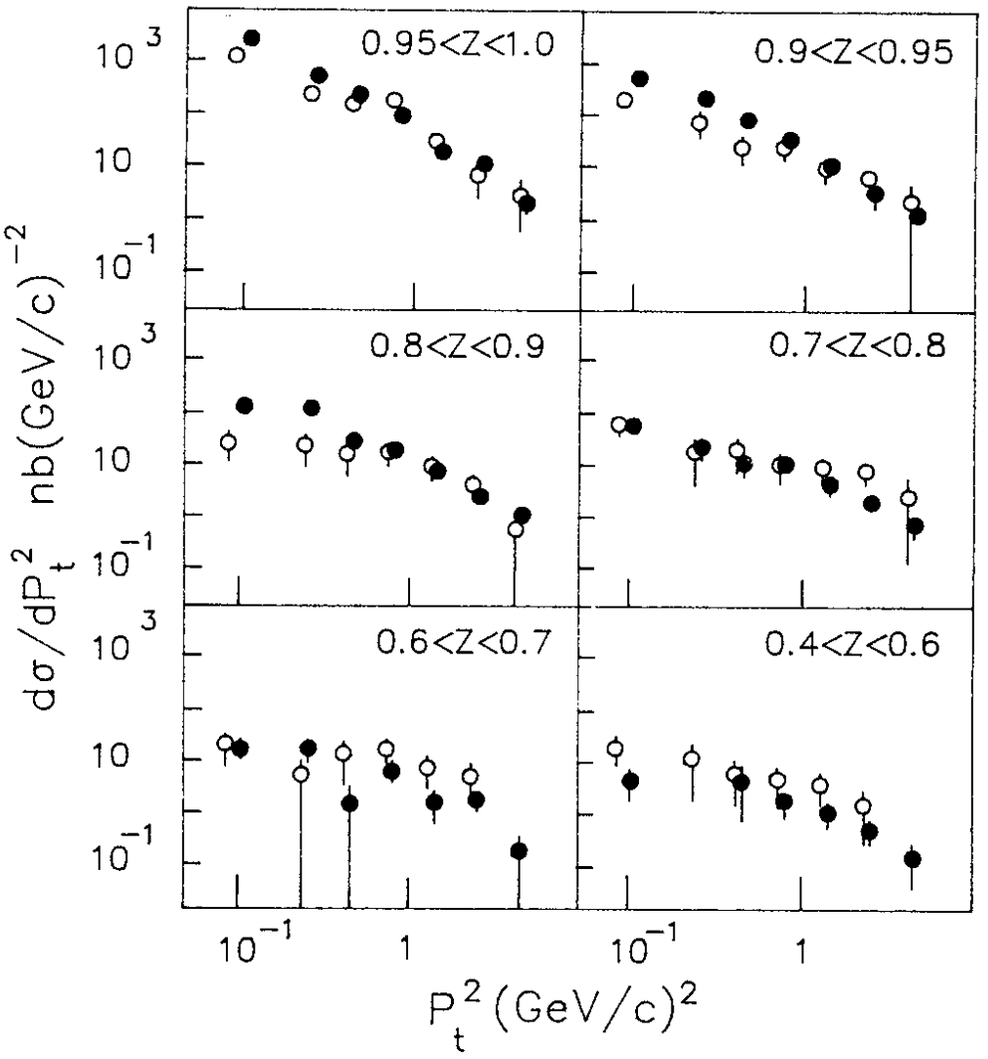
0.95<Z<1.0
0.9<Z<0.95
0.8<Z<0.9
0.7<Z<0.8
0.6<Z<0.7
0.4<Z<0.6
10^3
10
10^{-1}
1
$d\sigma/dP_t^2$ nb(GeV/c)$^{-2}$
P_t^2 (GeV/c)^2

Fig.3

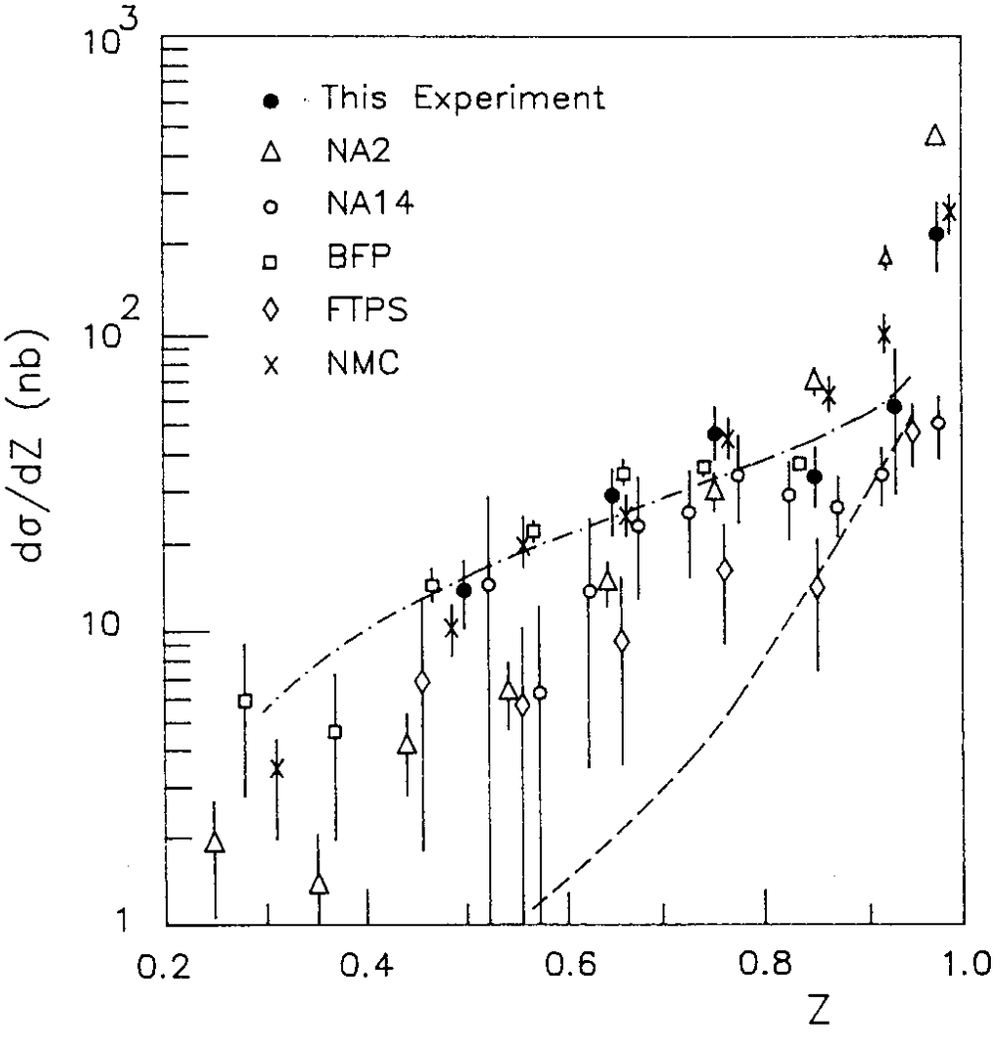
10^3
10^2
10
1
dσ/dZ (nb)
This Experiment
NA2
NA14
BFP
FTPS
NMC
0.2
0.4
0.6
0.8
1.0
Z

Fig.4

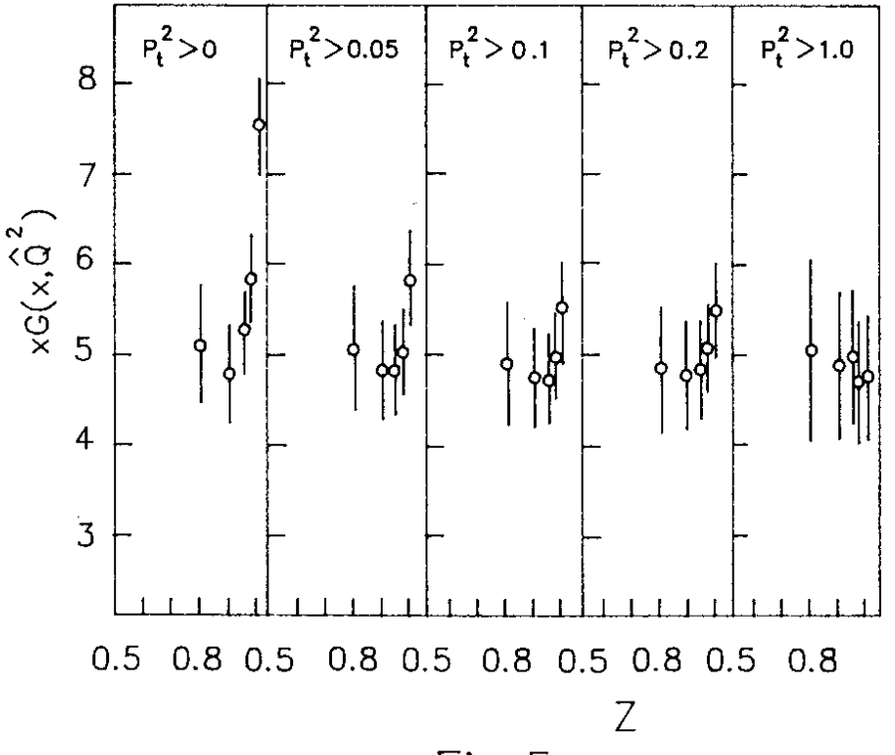
$P_t^2 > 0$
$P_t^2 > 0.05$
$P_t^2 > 0.1$
$P_t^2 > 0.2$
$P_t^2 > 1.0$
$xG(x,\hat{Q}^2)$
8
7
6
5
4
3
0.5 0.8 0.5 0.8 0.5 0.8 0.5 0.8 0.5 0.8
Z

Fig.5

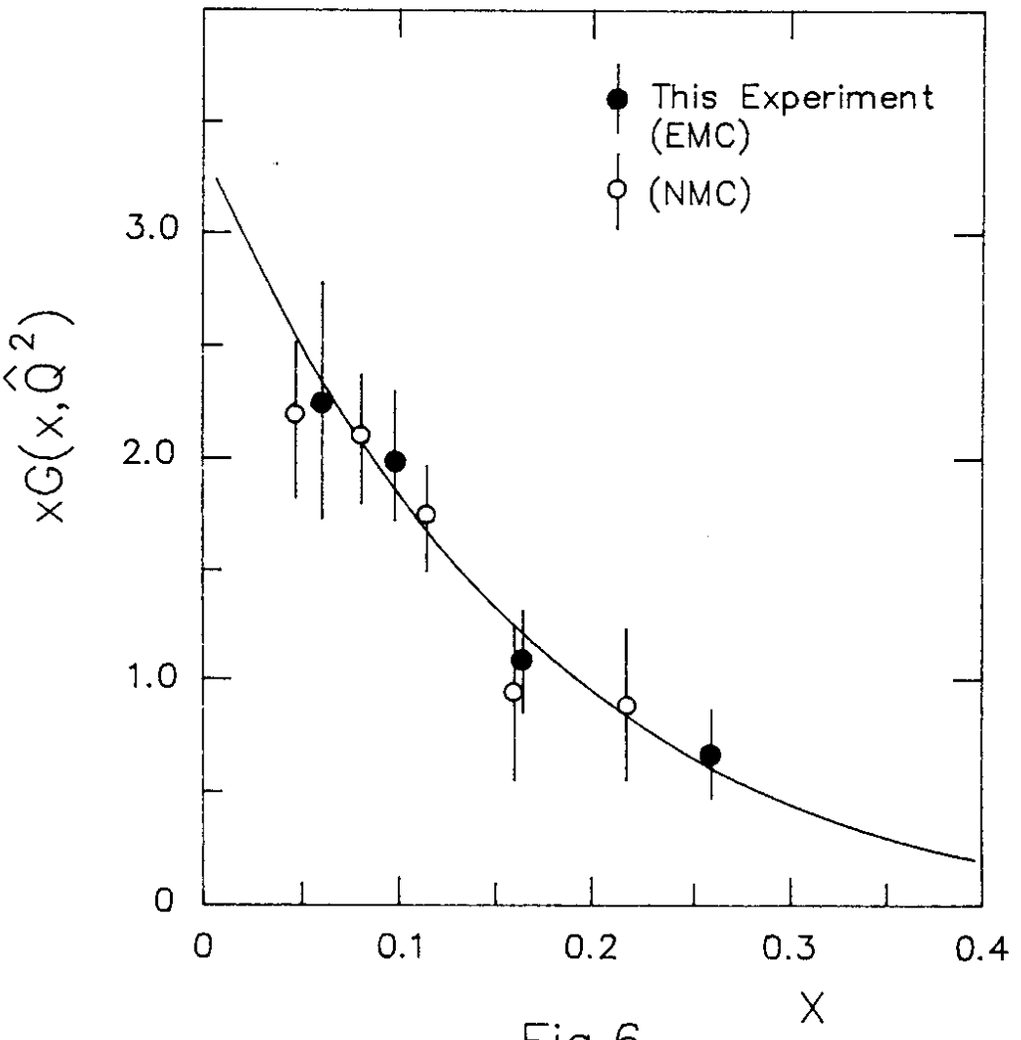

Fig.6

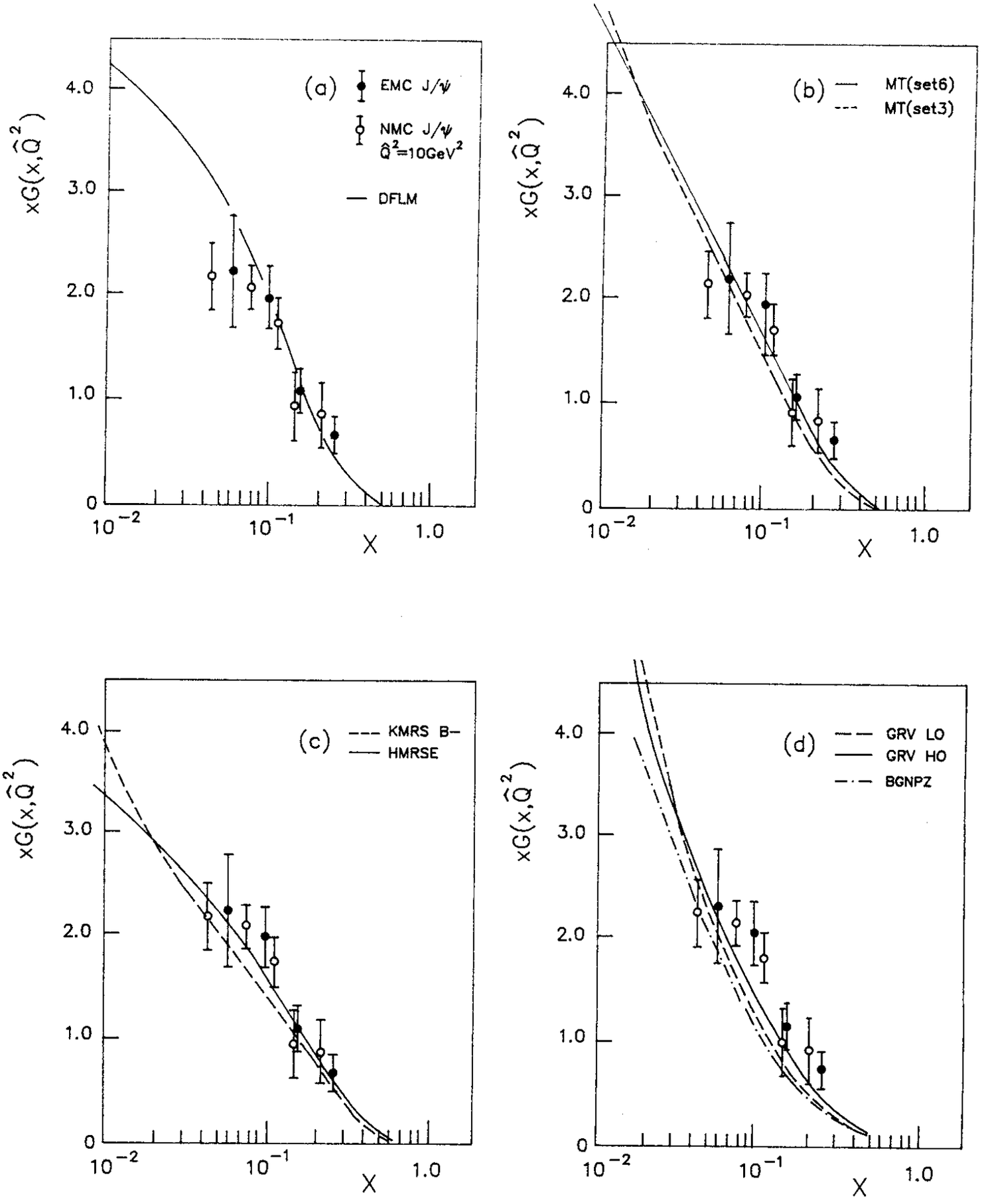
(a)
EMC J/ψ
NMC J/ψ
$\hat{Q}^2$=10GeV^2
DFLM
(b)
MT(set6)
MT(set3)
(c)
KMRS B−
HMRSE
(d)
GRV LO
GRV HO
BGNPZ
xG(x,$\hat{Q}^2$)
X
4.0
3.0
2.0
1.0
0
10^{-2}
10^{-1}
1.0

Fig. 7